# Single-Chain $\beta$ -D-Glycopyranosylamides of Unsaturated Fatty Acids: Self-Assembly Properties and Applications to Artificial Cell Development

Published as part of The Journal of Physical Chemistry virtual special issue "Young Scientists". Ahanjit Bhattacharya, \* Roberto J. Brea, \* Jing-Jin Song, \* Rupak Bhattacharya, \* Sunil K. Sinha, \* and Neal K. Devaraj\*,†©

Supporting Information

ABSTRACT: Amphiphilic molecules undergo self-assembly in aqueous medium to yield various supramolecular structures depending on their chemical structure and molecular geometry. Among these, lamellar membrane-bound vesicles are of special interest due to their resemblance to cellular membranes. Here we describe the self-assembly of singlechain amide-linked amphiphiles derived from  $\beta$ -D-galactopyr-



anosylamine and various unsaturated fatty acids into vesicles. In contrast, the analogous amphiphiles derived from  $\beta$ -Dglucopyranosylamine self-assemble into nanotubes. Fluorescence spectroscopy, X-ray diffraction, and differential scanning calorimetry are used to determine various physical parameters pertinent to the self-assembly process. The vesicular architecture is characterized using optical microscopy and transmission electron microscopy. Moreover, we show that the vesicles derived from these amphiphiles can encapsulate molecules of various sizes and host model biochemical reactions. Our work demonstrates that single-chain glycolipid-based amphiphiles could serve as robust building blocks for artificial cells and have potential applications in drug delivery and microreactor design.

## **■ INTRODUCTION**

Amphiphilic molecules self-assemble in aqueous medium to form supramolecular aggregates belonging to various lyotropic mesophases. Molecular geometry and functional groups on an amphiphile are the primary determinants of what kind of aggregate it will form. Glycolipids are an important class of amphiphiles that exhibit a wide variety of structural polymorphism depending on the molecular architecture. 1,2 These amphiphiles are characterized by a monosaccharide or oligosaccharide headgroup and a hydrophobic tail often originating from the condensation of fatty acids. Glycolipids play important roles in maintaining the stability of cellular membranes as well as serving as markers for cellular recognition. Despite their ubiquity, the structure-function relationship of glycolipids with respect to membrane formation is relatively less explored and requires detailed biophysical studies. Glycolipids derived from various microorganisms have been considered for applications as economic and environment-friendly biosurfactants.<sup>3,4</sup> Moreover, there is a significant interest in developing

ids for obtaining novel structural assemblies. workers have contributed extensively to the erization of self-assembled structures like s<sup>5</sup> and hydrogels.<sup>6</sup>

reported on the discovery of a new class of galactopyranose-derived single-chain amphiphiles (SCAs) that spontaneously self-assemble in water to form micron-sized vesicles. Unlike fatty-acids, β-D-galactopyranose-derived SCAs form membranes over a broad range of pH values and even in the presence of free divalent metal cations. With respect to being a building block for vesicles, the SCAs offer significant advantages and unique properties compared with phospholipids. For example, the semipermeable nature of the membranes derived from SCAs enables internal biochemical reactions such as rolling circle amplification (RCA) of DNA, even when precursors such as dNTPs are supplied externally. All of these features make them a powerful model system for the study and construction of advanced synthetic cells.

Here we describe the design, synthesis, and characterization of a collection of  $\beta$ -D-galactopyranosylamides derived from various unsaturated fatty acids, which spontaneously self-assemble to form membrane-bound vesicles (Figure 1a). We studied the glycolipids derived from oleic acid (GOA; 18:1,  $\omega$ 9), palmitoleic acid (GPOA; 16:1,  $\omega$ 7), and myristoleic acid (GMOA; 14:1,  $\omega$ 5) using various physical techniques and showed that all of them form highly stable vesicles in aqueous medium (Figure 1b). In contrast, we observed that the corresponding

Received: February 1, 2019 Revised: March 21, 2019 Published: April 9, 2019



pdfelement

The Trial Version

<sup>&</sup>lt;sup>†</sup>Department of Chemistry and Biochemistry, University of California, San Diego, La Jolla, California 92093, United States \*Department of Physics, University of California, San Diego, La Jolla, California 92093, United States

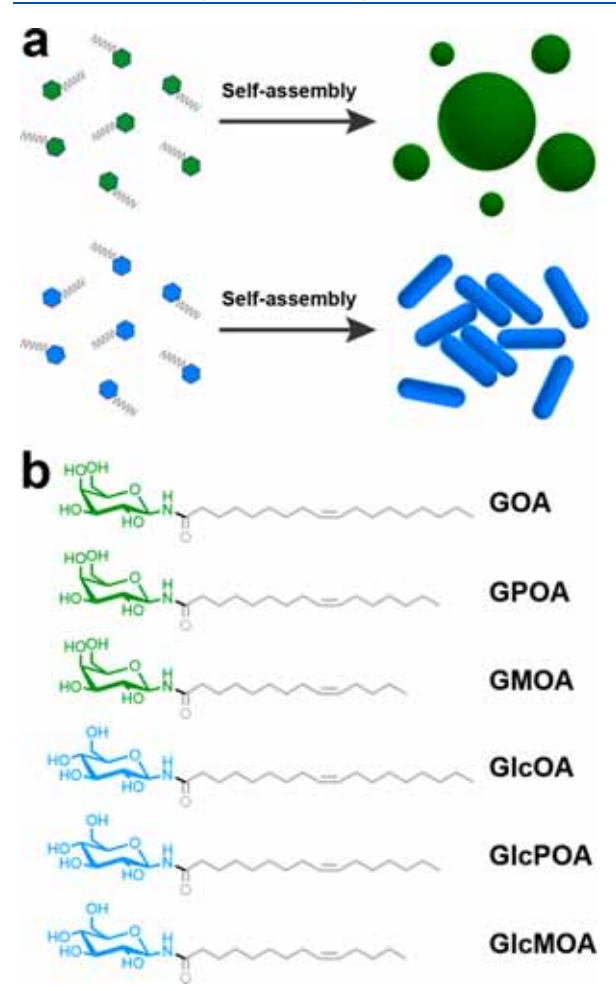


Figure 1. Self-assembled structures from single-chain glycopyranosyl amphiphiles. (a) Schematic representation of the formation of vesicles (top) from alkyl β-D-galactopyranosylamides and nanotubes (bottom) from alkyl β-D-galactopyranosylamides. (b) Structures of all amphiphiles used in this study (GOA: N-oleoyl β-D-galactopyranosylamine, GPOA: N-palmitoleoyl β-D-galactopyranosylamine, GMOA: N-myristoleoyl β-D-galactopyranosylamine, GlcOA: N-palmitoleoyl β-D-glucopyranosylamine, GlcPOA: N-palmitoleoyl β-D-glucopyranosylamine, GlcPOA: N-myristoleoyl β-D-glucopyranosylamine).

amphiphiles derived from  $\beta$ -D-glucopyranosylamine (GlcOA, GlcPOA, GlcMOA) form nanotubes in aqueous medium (Figure 1b), in good agreement with previous reports. Our results suggest that there is a strong correlation between the molecular structure and self-assembly properties of single-chain glycolipids, and their detailed physical studies may lead to the design of novel glycolipid amphiphiles and applications in membrane mimetic chemistry.

# EXPERIMENTAL SECTION

pdfelement
The Trial Version

md Materials. Commercially available  $\beta$ -D-amine and  $\beta$ -D-glucopyranosylamine were used om Carbosynth. Oleic acid (OA), O-(7-yl)-1,1,3,3-tetramethyl-uronium hexafluoro-TU), N,N-diisopropylethylamine (DIPEA), mamide (DMF), 8-hydroxypyrene-1,3,6-trisultonic acid (HPTS), 4-(2-hydroxyethyl)piperazine-1-ethanesul-

fonic acid (HEPES) sodium salt, Tween 80, chloroform,  $\beta$ galactosidase (E. coli overproducer, Roche) and 4-methylumbelliferyl  $\beta$ -D-galactopyranoside (MUG) were obtained from Sigma-Aldrich. Palmitoleic acid (POA) and myristoleic acid (MOA) were obtained from Cayman Chemicals. Proteinase K was obtained from New England Biolabs. Texas Red 1,2dihexadecanoyl-sn-glycero-3-phosphoethanolamine, triethylammonium salt (Texas Red DHPE) was purchased from Biotium. N,N-Dimethyl-6-dodecanoyl-2-naphthylamine (Laurdan) was obtained from Chemodex. Deuterated methanol (CD3OD) was purchased from Cambridge Isotope Laboratories. All mixtures of solvent mixtures for chromatographic separation are reported in terms of v/v ratios. An Eclipse Plus C8 analytical column was used for HPLC analyses. A Zorbax SB-C18 semipreparative column was used for purification by HPLC. The gradients are designated as ratios of Phase A/Phase B, where Phase A is composed of H2O with 0.1% formic acid and Phase B is composed of MeOH with 0.1% formic acid. Nuclear magnetic resonance (<sup>1</sup>H and <sup>13</sup>C NMR) spectra were acquired on a Varian VX-500 MHz instrument. High-resolution mass spectra (HR-MS) were obtained at the Molecular Mass Spectrometry Facility (MMSF) of the University of California, San Diego. A NanoDrop 2000C spectrophotometer was used for UV-vis measurements. Microscopy was carried out using an Olympus BX51 optical microscope and a Carl Zeiss Axio Observer Z1 spinning-disk confocal microscope.

Synthesis of Alkyl  $\beta$ -Glycopyranosylamides. Alkyl  $\beta$ -glycopyranosylamides (GOA, GPOA, GMOA, GlcOA, GlcPOA, GlcMOA) were synthesized according to Scheme S1.

N-Oleoyl  $\beta$ -D-Galactopyranosylamine (**GOA**). Oleic acid (25.9 mg, 91.6  $\mu$ mol) was dissolved in DMF (916  $\mu$ L) and stirred at 0 °C. After this, HATU (38.3 mg, 100.8  $\mu$ mol) and DIPEA (17.6 µL, 100.8 µmol) were added, respectively. After stirring for ~10 min,  $\beta$ -D-galactopyranosylamine (16.4 mg, 91.6  $\mu$ mol) was added. Stirring was continued for 1 h at rt, and the organic solvents were removed in vacuo. The yellow residue was dissolved in 500 µL of MeOH, filtered, and purified using HPLC. 36.8 mg of GOA was obtained as a white solid powder (91%). <sup>1</sup>H NMR (CD<sub>3</sub>OD, 500.13 MHz,  $\delta$ ): 5.44–5.25 (m, 2H,  $2 \times CH$ ), 4.84–4.83 (m, 1H, 1 × CH), 3.88 (d, J = 3.1 Hz, 1H, 1  $\times$  CH), 3.74–3.63 (m, 2H, 2  $\times$  CH), 3.61–3.47 (m, 3H, 1  $\times$  CH  $+1 \times CH_2$ ), 2.34–2.16 (m, 2H, 1 × CH<sub>2</sub>), 2.13–1.91 (m, 4H, 2  $\times$  CH<sub>2</sub>), 1.69–1.55 (m, 2H, 1  $\times$  CH<sub>2</sub>), 1.41–1.24 (m, 20H, 10  $\times$  $CH_2$ ), 0.90 (t, J = 6.8 Hz, 3H,  $1 \times CH_3$ ). <sup>13</sup>C NMR (CD<sub>3</sub>OD, 125.77 MHz,  $\delta$ ): 177.3, 130.9, 130.8, 81.5, 78.2, 75.8, 71.3, 70.5, 62.5, 37.2, 33.1, 30.9, 30.9, 30.6, 30.5, 30.4, 30.3, 30.3, 30.2, 28.2, 28.1, 26.6, 23.7, 14.4. HR-MS (ESI-TOF) calculated for  $[C_{24}H_{45}NO_6Na]$  ([M + Na]<sup>+</sup>) 466.3139, found 466.3139.

*N-Palmitoleoyl* β-*D-Galactopyranosylamine* (*GPOA*). A solution of POA (15.9 μL, 55.8 μmol) in DMF (558 μL) was stirred at 0 °C, following which HATU (23.3 mg, 61.4 μmol) and DIPEA (38.9 μL, 223.3 μmol) were added, respectively. After stirring for 10 min, β-*D*-galactopyranosylamine (10.0 mg, 55.8 μmol) was added. The reaction was continued at rt for 1 h, and the solvents were removed in vacuo. The yellowish residue was dissolved in 500 μL of MeOH, filtered, and purified on HPLC. 20.7 mg of GPOA was afforded as a white solid powder (89%). <sup>1</sup>H NMR (CD<sub>3</sub>OD, 500.13 MHz, δ): 5.42–5.27 (m, 2H, 2 × CH), 4.85 (d, J = 8.6 Hz, 1H, 1 × CH), 3.88 (dd,  $J_1 = 3.1$  Hz,  $J_2 = 1.1$  Hz, 1H, 1 × CH), 3.73–3.63 (m, 2H, 2 × CH), 3.60–3.47 (m, 3H, 1 × CH + 1 × CH<sub>2</sub>), 2.34–2.17 (m, 2H, 1 × CH<sub>2</sub>), 2.10–1.98 (m, 4H, 2 × CH<sub>2</sub>), 1.71–1.57 (m, 2H, 1 × CH<sub>2</sub>), 1.40–1.24 (m, 16H, 8 × CH<sub>2</sub>), 0.91 (t, J = 6.9 Hz, 3H, 1 × CH<sub>3</sub>).

 $^{13}$ C NMR (CD<sub>3</sub>OD, 125.77 MHz, δ): 177.3, 130.9, 130.8, 81.5, 78.2, 75.8, 71.3, 70.4, 62.5, 37.2, 33.0, 30.9, 30.4, 30.4, 30.3, 30.1, 28.2, 26.7, 23.8, 14.5. HR-MS (ESI-TOF) calculated for [C<sub>22</sub>H<sub>41</sub>NO<sub>6</sub>Na] ([M + Na]<sup>+</sup>) 438.2826, found 438.2821.

N-Myristoleoyl  $\beta$ -D-Galactopyranosylamine (**GMOA**). A solution of MOA (7.0  $\mu$ L, 27.9  $\mu$ mol) in DMF (279  $\mu$ L) was stirred at 0 °C. Next, HATU (11.7 mg, 30.7  $\mu$ mol) and DIPEA  $(19.4 \,\mu\text{L}, 111.6 \,\mu\text{mol})$  were added successively. After stirring for 10 min,  $\beta$ -D-galactopyranosylamine (5.0 mg, 27.9  $\mu$ mol) was added. Stirring was continued for 1 h at rt, and then the solvents were removed in vacuo. The yellowish residue was dissolved in 250  $\mu$ L of MeOH, filtered, and purified by HPLC. 8.0 mg of GMOA was obtained as a white solid (74%). <sup>1</sup>H NMR (CD<sub>3</sub>OD, 500.13 MHz,  $\delta$ ): 5.42–5.29 (m, 2H, 2 × CH), 4.85  $(d, J = 8.6 \text{ Hz}, 1\text{H}, 1 \times \text{CH}), 3.88 (dd, J_1 = 3.1 \text{ Hz}, J_2 = 1.1 \text{ Hz},$  $1H, 1 \times CH), 3.73 - 3.64 (m, 2H, 2 \times CH), 3.60 - 3.48 (m, 3H, 1)$  $\times$  CH + 1  $\times$  CH<sub>2</sub>), 2.33–2.19 (m, 2H, 1  $\times$  CH<sub>2</sub>), 2.11–1.98 (m, 4H,  $2 \times CH_2$ ), 1.71-1.56 (m, 2H,  $1 \times CH_2$ ), 1.41-1.29 (m, 12H,  $6 \times \text{CH}_2$ ), 0.91 (t, J = 7.1 Hz, 3H,  $1 \times \text{CH}_3$ ). <sup>13</sup>C NMR (CD<sub>3</sub>OD, 125.77 MHz, δ): 177.3, 130.8, 130.8, 81.5, 78.2, 75.8, 71.3, 70.4, 62.5, 37.2, 33.2, 30.9, 30.4, 30.4, 30.2, 28.1, 27.9, 26.7, 23.4, 14.4. HR-MS (ESI-TOF) calculated for  $[C_{20}H_{37}NO_6Na]$  $([M + Na]^{+})$  410.2513, found 410.2508.

N-Oleoyl  $\beta$ -D-Glucopyranosylamine (**GlcOA**). Oleic acid solution (25.9 mg, 91.6  $\mu$ mol) in DMF (916  $\mu$ L) was stirred at 0  $^{\circ}$ C, and then HATU (38.3 mg, 100.8  $\mu$ mol) and DIPEA (17.6  $\mu$ L, 100.8  $\mu$ mol) were added successively. After stirring for 10 min,  $\beta$ -D-glucopyranosylamine (16.4 mg, 91.6  $\mu$ mol) was added. Stirring was continued for 1 h at rt, followed by the removal of solvents in vacuo. The resulting yellowish residue was dissolved in 500  $\mu$ L of MeOH, filtered, and purified on HPLC. 34.3 mg of GlcOA was obtained as a white solid powder (85%). <sup>1</sup>H NMR (CD<sub>3</sub>OD, 500.13 MHz,  $\delta$ ): 5.41–5.26 (m, 2H, 2 × CH), 4.89  $(d, J = 9.1 \text{ Hz}, 1\text{H}, 1 \times \text{CH}), 3.82 \text{ (dd}, J_1 = 12.0 \text{ Hz}, J_2 = 2.1 \text{ Hz},$ 1H, 1 × CH), 3.65 (dd,  $J_1$  = 12.0 Hz,  $J_2$  = 5.1 Hz, 1H, 1 × CH), 3.39 (t, J = 8.8 Hz, 1H, 1 × CH), 3.37–3.32 (m, 1H, 1 × CH), 3.30-3.20 (m, 2H,  $1 \times CH_2$ ), 2.24 (td,  $J_1 = 7.5$  Hz,  $J_2 = 4.1$  Hz,  $2H, 1 \times CH_2$ ), 2.10-1.96 (m,  $4H, 2 \times CH_2$ ), 1.72-1.52 (m, 2H,  $1 \times CH_2$ ), 1.39–1.24 (m, 20H,  $10 \times CH_2$ ), 0.90 (t, J = 6.8 Hz, 3H, 1 × CH<sub>3</sub>). <sup>13</sup>C NMR (CD<sub>3</sub>OD, 125.77 MHz,  $\delta$ ): 177.3, 130.9, 130.8, 81.0, 79.6, 79.0, 73.9, 71.4, 62.6, 37.1, 33.1, 30.9, 30.9, 30.7, 30.5, 30.4, 30.4, 30.4, 30.3, 28.2, 28.1, 26.6, 23.8, 14.5. HR-MS (ESI-TOF) calculated for  $[C_{24}H_{44}NO_6]$  ( $[M-H]^-$ ) 442.3174, found 442.3175.

*N-Palmitoleoyl* β-D-Glucopyranosylamine (**GlcPOA**). A solution of POA (5.7 mg, 22.4 μmol) in DMF (500 μL) was stirred at 0 °C; then, HATU (13.9 mg, 36.6 μmol) and DIPEA (7.8 μL, 44.8 μmol) were added consecutively. After stirring for 10 min, β-D-glucopyranosylamine (8.0 mg, 44.7 μmol) was added. Stirring was continued for 2 h at rt, followed by the removal of solvents in vacuo. The resulting yellowish residue was dissolved in 300 μL of MeOH, filtered, and purified on HPLC. 3.9 mg of **GlcPOA** was obtained as a white solid powder (42%). <sup>1</sup>H NMR (CD<sub>3</sub>OD, 500.13 MHz, δ): 5.43–5.26 (m, 2H, 2 × CH), 4.89 (d, J = 9.1 Hz, 1H, 1 × CH), 3.82 (dd, J<sub>1</sub> = 12.0 Hz, J<sub>2</sub> = 2.2 Hz, 1H, 1 × CH), 3.65 (dd, J<sub>1</sub> = 11.9 Hz, J<sub>2</sub> = 5.1 Hz, 1H, 1

= 8.8 Hz, 1H, 1 × CH), 3.35–3.32 (m, 1H, 0.5 26 (m, 1H, 0.5 × CH<sub>2</sub>), 3.23 (t, J = 9.1 Hz, 1H, .16 (m, 2H, 1 × CH<sub>2</sub>), 2.10–1.98 (m, 4H, 2 × (m, 2H, 1 × CH<sub>2</sub>), 1.40–1.26 (m, 16H, 8 × 7.0 Hz, 3H, 1 × CH<sub>3</sub>). The constant of the constan

14.5. HR-MS (ESI-TOF) calculated for  $[C_{22}H_{41}NO_6Na]^+$  ([M + Na]<sup>+</sup>) 438.2826, found 438.2823.

N-Myristoleoyl  $\beta$ -D-Glucopyranosylamine (**GlcMOA**). MOA (10.4 mg, 46.0  $\mu$ mol) was dissolved in DMF (700  $\mu$ L) by stirring at 0 °C. Next, HATU (27.6 mg, 72.6 µmol) and DIPEA (16.0  $\mu$ L, 92.0  $\mu$ mol) were added successively. After stirring for 10 min,  $\beta$ -D-glucopyranosylamine (16.5 mg, 92.2  $\mu$ mol) was added. Stirring was continued for 1.5 h at rt, followed by the removal of solvents in vacuo. The resulting yellow residue was dissolved in 400  $\mu$ L of MeOH, filtered, and purified on HPLC. 12.9 mg of GlcMOA was obtained as a white solid powder (73%). <sup>1</sup>H NMR (CD<sub>3</sub>OD, 500.13 MHz,  $\delta$ ): 5.42–5.25 (m, 2H, 2 × CH), 4.89 (d, J = 9.1 Hz, 1H, 1 × CH), 3.82 (dd,  $J_1$ = 12.0 Hz,  $J_2$  = 2.2 Hz, 1H, 1 × CH), 3.65 (dd,  $J_1$  = 11.9 Hz,  $J_2$  = 5.1 Hz, 1H, 1 × CH), 3.39 (t, J = 8.8 Hz, 1H, 1 × CH<sub>3</sub>), 3.36–  $3.32 \text{ (m, 1H, } 0.5 \times \text{CH}_2), 3.30 - 3.26 \text{ (m, 1H, } 0.5 \times \text{CH}_2), 3.23$  $(t, J = 9.1 \text{ Hz}, 1H, 1 \times \text{CH}), 2.32 - 2.16 \text{ (m, 2H, } 1 \times \text{CH}_2), 2.12 -$ 1.94 (m, 4H,  $2 \times CH_2$ ), 1.71–1.52 (m, 2H,  $1 \times CH_2$ ), 1.38– 1.29 (m, 12H,  $6 \times CH_2$ ), 0.91 (t, J = 7.1 Hz, 3H,  $1 \times CH_3$ ). <sup>13</sup>C NMR (CD<sub>3</sub>OD, 125.77 MHz, δ): 177.3, 130.8, 130.8, 81.0, 79.6, 79.0, 73.9, 71.3, 62.6, 37.1, 33.1, 30.8, 30.4, 30.4, 30.2, 28.1, 27.9, 26.6, 23.4, 14.4. HR-MS (ESI-TOF) calculated for  $[C_{20}H_{37}NO_6Na]^+$  ( $[M + Na]^+$ ) 410.2513, found 410.2509.

Critical Aggregation Concentration Determination. The critical aggregation concentrations (cac's) of the various lipids used in this study were estimated using a method based on the solvatochromic fluorescent dye Laurdan. Laurdan shows a sharp change in the value of generalized polarization (GP) at or near the cac (or critical micelle concentration (cmc)) value of an amphiphile. Initially, a dispersion of the lipid was prepared in Milli-Q H<sub>2</sub>O by hydration of a thin film, followed by sonication. Afterward, various solutions (20  $\mu$ L each) were prepared by the dilution of the concentrated dispersions with Milli-Q H<sub>2</sub>O. The samples were kept at 37 °C for 1 h, following which 0.25  $\mu$ L of Laurdan (100  $\mu$ M in EtOH) was added to each and mixed by gentle tapping. Then, the samples were transferred to a 384-well plate and analyzed on a Tecan Infinite plate reader at 37 °C. The samples were excited at 364 nm, and emission spectra were acquired over 430-500 nm. The GP was calculated as follows

$$GP = \frac{I_{440} - I_{490}}{I_{440} + I_{490}} \tag{1}$$

where  $I_{440}$  and  $I_{490}$  stands for the fluorescence intensities at the wavelengths 440 and 490 nm, respectively. The values of GP were plotted against the lipid concentrations for each dilution.

Transmission Electron Microscopy Studies. Micrographs were recorded on an FEI Tecnai Sphera microscope operating at 200 kV and equipped with a LaB<sub>6</sub> electron gun using the standard cryotransfer holders developed by Gatan. Copper grids (Formvar/carbon-coated, 400 mesh copper) were glow discharged at 20 mA for 1.5 min. After this, 3.5  $\mu$ L of a dispersion of the glycolipid (GOA, GPOA, GMOA, and GlcOA) in H<sub>2</sub>O was added to the grid surface and allowed to sit for ~10 s. It was washed with 10 drops of ultrapure H<sub>2</sub>O and subsequently stained with three drops of 1% uranyl acetate. The staining was carried out for ~10 s before blotting with filter paper. Following this, samples were imaged by transmission electron microscopy (TEM).

X-ray Diffraction and Electron Density Profile Measurements. Glycolipid multilayers were deposited on silicon [100] substrates by following the reported protocols. A concentrated solution (10 mM) of the glycolipid (GOA, GPOA,



GMOA or GlcOA) in methanol was used to drop-coat the film on freshly cleaned (MeOH/deionized H<sub>2</sub>O) hydrophilic silicon substrate. The evaporation rate of the mixed solvent was controlled to obtain a uniform coated film over 10 × 10 mm of surface. The deposited films were then put in high vacuum  $(10^{-3})$ Torr) for >12 h to remove trapped solvents. To obtain a welloriented lipid multilayer, the dried films were then rehydrated under 100% relative humidity (RH) at 50 °C. A slow and steady humidity incubation for >24 h produced a well-oriented smectic lipid multilayer membrane with long-range correlation among consecutive layers. Subsequently, samples were stored in sealed boxes at room temperature and under RH of ~98% using saturated salt (K<sub>2</sub>SO<sub>4</sub>) solution vapor. X-ray diffraction (XRD) measurements were carried out at our in-house XRD setup (D8 Discover, Bruker) consisting of a four-circle goniometer and a Cu K $\alpha$  (8.04 keV,  $\lambda \approx 1.54$  Å) source. A special sealed humidity chamber was used to control precisely the RH of the sample.

*X-ray Diffraction Intensity Profiles.* For the representation of the typical XRD intensity profile of the glycolipid samples, we have plotted integrated intensity as a function of the transferred wave vector  $(q_x)$ 

$$q_z = \frac{4\pi}{\lambda} \sin \theta \tag{2}$$

where  $\theta$  is the grazing angle of incidence and  $\lambda$  stands for the wavelength of the incident X-ray.

Relative Electron Density Profiles. We obtained a set of Bragg peaks from the XRD profile, indicating long-range ordering in the glycolipid multilayers deposited on the substrate. To quantify further, we determined the relative electron density profile (EDP) of the stacked multilayers. The EDP can be can generated from the XRD intensity profile using the following equation

$$\rho_{\text{relative}}(z) = \frac{2}{d} \sum_{n} \nu_{n} |F_{n}| \cos\left(\frac{2\pi nz}{d}\right)$$
(3)

where d represents the d spacing of the stacked multilayer, n is the Bragg peak order number,  $v_n$  is the phase factor, and  $F_n = n\sqrt{I_n}$ , where  $I_n$  represents the integrated intensity of the nth order peak and the factor n includes the Lorentz correction factor apart from a multiplicative constant. In practice, we considered the first six Bragg peaks from the intensity profile. The phase factors  $v_n$  were taken from those obtained from similar lipid multilayers utilizing the swelling method. <sup>10</sup> Because the EDPs of bilayers are assumed to be centrosymmetric, the phase's  $v_n$  can only be of combination of +1 or -1. The relative EDPs are indeterminate to the extent of an overall scale factor and a shift arising from n=0 Fourier coefficient in eq 3. The corresponding EDP data allowed us to estimate the membrane thickness (head-to-head distance of the lipid bilayer) for the glycolipids under consideration.

**Differential Scanning Calorimetry Measurements.** Differential scanning calorimetry (DSC) was used to study the phase-transition behavior of the glycolipids. All thermograms

a Microcal VP-Capillary DSC (Ward Lab, The Institute). GOA, GPOA, GMOA, GlcOA, lcMOA dispersions were prepared in Milli-Q ations of 0.5, 1.0, 2.0, 0.5, 0.5, and 1.5 mM, volume of sample used for the analyses was e scan rate for each sample was 30 °C/h. The gain settings were set to "high". Background subtraction and

processing of the thermograms were carried out using Microcal Origin Software provided by the manufacturer.

**Encapsulation Experiments.** *Encapsulation of HPTS* (*Pyranine*) *Dye.* A thin lipid film was prepared on the walls of a glass vial by evaporating a solution of **GOA** in CHCl<sub>3</sub>/MeOH (2:1). Hydration of the lipid film was carried out by vortexing with 60  $\mu$ L of a solution containing 1 mM HPTS, 0.2 mM Tween 80, and 50 mM Tris (pH 8.0). The final concentration of **GOA** in the dispersion was 3.0 mM. The dispersion was further tumbled at 37 °C for 1 h. The unencapsulated dye was removed by washing the dispersion with 50 mM Tris (pH 8.0) using a spin filter (300 kDa molecular weight cutoff (MWCO), Pall Corporation). A small volume of the retentate was examined by spinning-disk confocal microscopy, and large number of vesicles were observed with HPTS encapsulated.

Encapsulation of Fluorescently Labeled Dextran. A thin lipid film was prepared on the walls of a glass vial by evaporating a solution of GOA in CHCl $_3$ /MeOH (2:1). Hydration of the lipid film was carried out by vortexing with 60  $\mu$ L of a solution containing 2 mg/mL fluorescein isothiocyanate (FITC)-labeled dextran (3–5 kDa, Sigma-Aldrich), 0.2 mM Tween 80, and 50 mM Tris (pH 8.0). The final concentration of GOA in the dispersion was 3 mM. The dispersion was tumbled at 37 °C for 1 h. The unencapsulated dextran was removed by washing the dispersion with 50 mM Tris (pH 8.0) using a spin filter (300 kDa MWCO, Pall Corporation). The washed vesicle dispersion was observed by spinning-disk confocal microscopy, and vesicles encapsulating labeled dextran were imaged.

Encapsulation of Fluorescently Labeled Oligonucleotide. A thin lipid film was prepared on the walls of a glass vial by evaporating a solution of GOA in CHCl<sub>3</sub>/MeOH (2:1). Hydration of the lipid film was carried out by vortexing with 60  $\mu$ L of a solution containing 50  $\mu$ M 5′-FAM dN<sub>20</sub> oligonucleotide (Sequence: 5′-FAM-TAATACGACTCACTATAGGG-3′, Integrated DNA Technologies), 0.2 mM Tween 80, and 50 mM Tris (pH 8.0). The final concentration of GOA in the dispersion was 3 mM. The dispersion was further tumbled at 37 °C for 2 h. The unencapsulated oligonucleotide was removed by washing the dispersion with 50 mM Tris (pH 8.0) using a spin filter (300 kDa MWCO, Pall Corporation). A small volume of the retentate was examined by spinning-disk confocal microscopy, and large number of vesicles were detected with the fluorescently labeled oligonucleotide encapsulated inside.

Encapsulation of Green Fluorescent Protein. A thin lipid film was prepared on the walls of a glass vial by evaporating a solution of GOA in CHCl<sub>3</sub>/MeOH (2:1). Hydration of the lipid film was carried out by vortexing with 60  $\mu$ L of a solution containing 8.33  $\mu$ M His<sub>6</sub>-sfGFP, 0.2 mM Tween 80, and 50 mM HEPES-K (pH 7.6). The final concentration of GOA in the dispersion was 3 mM. The dispersion was further tumbled at 37 °C overnight. The unencapsulated green fluorescent protein (GFP) was removed by washing the dispersion with 50 mM HEPES-K (pH 7.6) using a spin filter (300 kDa MWCO, Pall Corporation). A small volume of the retentate was examined by spinning-disk confocal microscopy, and large number of vesicles with GFP encapsulated were observed.

Activity of  $\dot{\beta}$ -Galactosidase in GOA Vesicles. A thin lipid film was prepared on the walls of a glass vial by evaporating a solution of GOA in CHCl<sub>3</sub>/MeOH (2:1). Hydration of the lipid film was carried out by vortexing with 60  $\mu$ L of a solution containing 50 U/mL  $\beta$ -galactosidase, 0.2 mM Tween 80, 1 mM MgCl<sub>2</sub>, 1 mM CaCl<sub>2</sub>, and 25 mM  $\beta$ -mercaptoethanol in 100 mM HEPES-K (pH 7.6). The final concentration of GOA in the

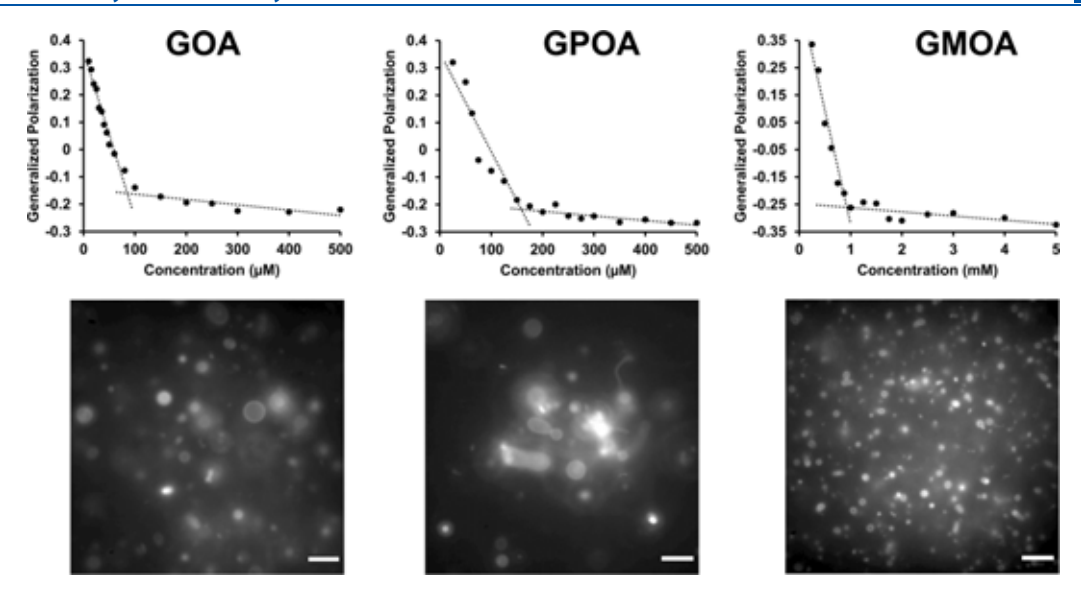


Figure 2. Critical aggregation concentration (cac) of various β-D-galactopyranosylamides. The cac values of GOA, GPOA, and GMOA were estimated using a method based on the fluorescence properties of the dye Laurdan. Representative plots are shown in the upper panel. In the lower panel, the images of the vesicles formed by the corresponding amphiphiles in water are given. All scale bars represent 10 μm. The membranes are stained with Texas Red DHPE.

dispersion was 3 mM. The dispersion was tumbled at 37 °C for 1.5 h. Following this, 2  $\mu$ L of proteinase K (20 mg/mL) was added, and the tumbling continued overnight at 37 °C. In the control experiment, an equal amount of proteinase K was added to the hydration buffer in the beginning. Twenty  $\mu$ L of the vesicle dispersion was taken, and 0.2  $\mu$ L of the fluorogenic substrate MUG (50 mM in DMSO) was added. The dispersions were immediately placed in a 384-well plate, and fluorescence ( $\lambda_{\rm ex}$ : 375 nm, bandwidth: 20 nm;  $\lambda_{\rm em}$ : 475 nm, bandwidth: 20 nm) was monitored every 30 s at 30 °C for 1 h.

#### ■ RESULTS AND DISCUSSION

Self-Assembly Behavior of  $\beta$ -D-Glycopyranosylamide **Amphiphiles.** We have recently demonstrated that N-oleoyl  $\beta$ -D-galactopyranosylamine (previously abbreviated as OGA; abbreviated in this work as GOA) self-assembles to form highly stable vesicles in aqueous medium. First, we asked if galactopyranose amphiphiles with shorter hydrophobic tails can also form membrane-bound vesicles. To address this question, we condensed the naturally occurring monounsaturated fatty acids POA (16:1,  $\omega$ 7) and MOA (14:1,  $\omega$ 5) with  $\beta$ -Dgalactopyranosylamine and synthesized the corresponding amides (GPOA and GMOA, respectively). Interestingly, we observed that GPOA and GMOA both self-assemble to form vesicles in aqueous medium. Using a method based on the fluorescence properties of the dye Laurdan, we estimated the cac for all three amphiphiles and obtained the values 0.079, 0.173, and 0.972 mM for GOA, GPOA, and GMOA, respectively (Figure 2, Table 1). The trend is consistent with a previous study on the dependence of cac on alkyl chain length. 11 We visualized



f micron-sized vesicles from each of these ptical microscopy using Texas Red DHPE as a (Figure 2). We further characterized the es formed from GOA, GPOA, and GMOA by transmission electron microscopy (TEM) and al compartments of the approximate size range

0.1 to 1  $\mu$ m (Figure 3a, Figure S2).

Table 1. Summary of the Physical Parameters of the Various Amphiphiles Used in This Work<sup>a</sup>

parameter	GOA	GPOA	GMOA	GlcOA
cac d spacing	0.079 mM 48.30 Å	0.173 mM 34.88 Å	0.972 mM 46.86 Å	47.53 Å
head-to-head distance	35.25 Å	26.16 Å	32.64 Å	35.00 Å
position of shoulder in the alkyl region	7.36 Å	4.67 Å		6.77 Å
$T_{ m m}$	37 °C	34 °C	30 °C	60 °C

"cac values are reported as the mean of values obtained from three independent measurements.

Next, we carried out the synthesis of N-oleoyl  $\beta$ -Dglucopyranosylamine (GlcOA). It was interesting to observe that GlcOA exclusively formed micron-sized nanotubes in aqueous medium (Figure 3b). TEM corroborated the nanotubular architecture for the corresponding self-assembled glycolipid structures (Figure 3b). The nanotubes possess welldefined hollow cylinders with inner diameters of ~70 nm and outer diameters of ~220 nm. Our observations are consistent with the previous report by Shimizu and coworkers. Furthermore, we also observed that the palmitoleoyl and myristoleoyl derivatives (GlcPOA and GlcMOA, respectively) also self-assemble to form micron-sized nanotubes in aqueous medium (Figure S3). It is interesting to note how variation in the monosaccharide can have drastic manifestations on the supramolecular assemblies of amphiphiles, which suggests the possibility for further expansion of supramolecular structures through headgroup modification.

**X-ray Diffraction Studies.** The XRD intensity profiles with respect to  $q_z$  for GOA, GMOA, GPOA, and GlcOA are provided in Figure 4. The presence of equidistant Bragg peaks indicates the formation of multilamellar structures by each of these lipids. As described in the Experimental Section, to characterize these assemblies, EDPs were constructed from intensities of the Bragg reflections using inverse Fourier transformation. Because of the

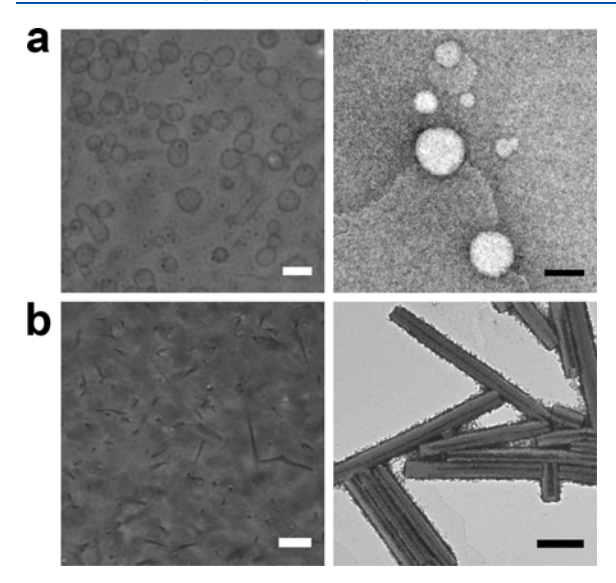
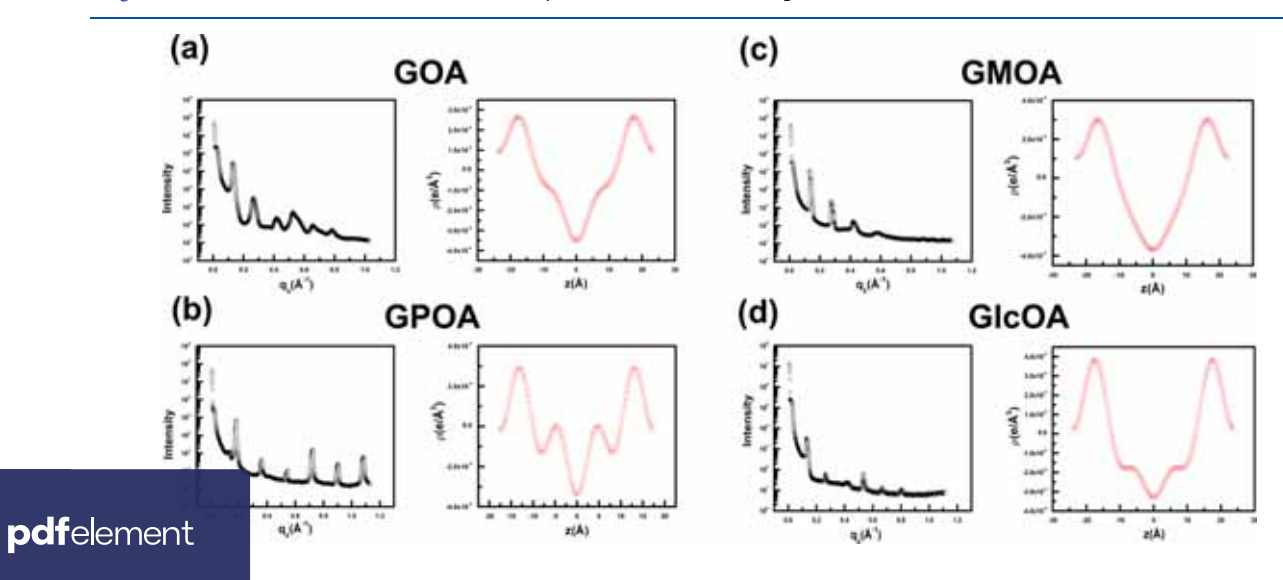


**Figure 3.** Comparison of self-assembled structures formed by **GOA** and **GlcOA**. (a) Optical microscopy (scale bar:  $5 \mu m$ ) and negative staining transmission electron microscopy (scale bar: 100 nm) images of **GOA** vesicles. (b) Optical microscopy (scale bar:  $5 \mu m$ ) and negative staining transmission electron microscopy (scale bar:  $1 \mu m$ ) images of **GlcOA** nanotubes.

symmetric nature of the bilayer leaflet, z=0 indicates the horizontal plane at the center of the bilayer. From the EDPs of different lipids, we estimated how the molecules align along the bilayer normal axis. We summarized the d spacing and head-to-head distances of the lipids in Table 1. The EDPs indicate that the folding of the alkyl chains varies across the four samples. In GOA, we observed a shoulder at 7.36 Å from the equatorial plane (Figure 4a). In the case of GPOA, the effect of chain folding was observed to be more pronounced, giving rise to a distinct shoulder peak at 4.67 Å from the equatorial plane (Figure 4b). In contrast, we did not observe any shoulder for

GMOA (Figure 4c). This is likely due to less splay in its alkyl chain, resulting in a nearly straight configuration of the latter. In qualitative terms, the EDP of GlcOA multilayers was observed to be similar to that of GOA, suggesting that in a multilayer structure the arrangement of the oleoyl chains is similar in these two lipids (Figure 4d). The observed differences (vesicles vs nanotubes) in the self-assembly properties of GOA and GlcOA in aqueous solution possibly stem from the nature of intermolecular hydrogen-bonding interactions between the headgroups.

Phase Transition Behavior. Transitions between various lyotropic phases are defining thermodynamic events for all amphiphiles. We sought to determine the behavior of the amphiphiles used in our study as a function of temperature. We analyzed aqueous dispersions of GOA, GPOA, GMOA, GlcOA, GlcPOA, and GlcMOA by DSC over a broad range of temperature (1-90 °C) and obtained the corresponding thermograms (Figure 5). All amphiphiles exhibited an asymmetric endothermic main transition peak, the maximum of which can be interpreted as the chain melting temperature  $(T_{\rm m})$  (Figure 5, Table 1). In addition, GOA exhibited a sharp, relatively narrow, and intense endothermic peak around 25 °C, preceding the peak corresponding to the main transition at 37 °C (Figure 5, Table 1). We propose that the aforementioned peak corresponds to a pretransition event, likely arising from a rearrangement from a subgel phase to a bilayer gel phase, as has been previously observed in the case of several bilayer membrane-forming lipids.  $^{12-14}$  Overall, the  $\beta$ -D-glucopyranosylamides exhibited significantly higher transition temperatures as compared with the corresponding  $\beta$ -D-galactopyranosylamides (Figure 5, Table 1). These differences likely arise from the more extensive intermolecular hydrogen bonding between the headgroups of glucose units in the former class. Interestingly, the  $T_{\rm m}$  value among the  $\beta$ -D-galactopyranosylamides varies as GOA (37 °C) > GPOA (34 °C) > GMOA (30 °C), whereas among  $\beta$ -D-glucopyranosylamides, the trend is reversed as GlcOA (60  $^{\circ}$ C) < GlcPOA (61  $^{\circ}$ C) < GlcMOA (62  $^{\circ}$ C). These trends suggest that the combined effect of the alkyl chain length and position of the cis-double bond have different manifes-



The Trial Version rization of the glycolipid amphiphiles used in this study by X-ray diffraction (XRD). Multilayer films of (a) GOA, (b) GPOA, (c) GLOA are analyzed by XRD at room temperature (~22 °C) and 98% relative humidity (RH). The XRD intensity profiles are displayed on the left, and the relative electron density profiles (EDPs) are displayed on the right.

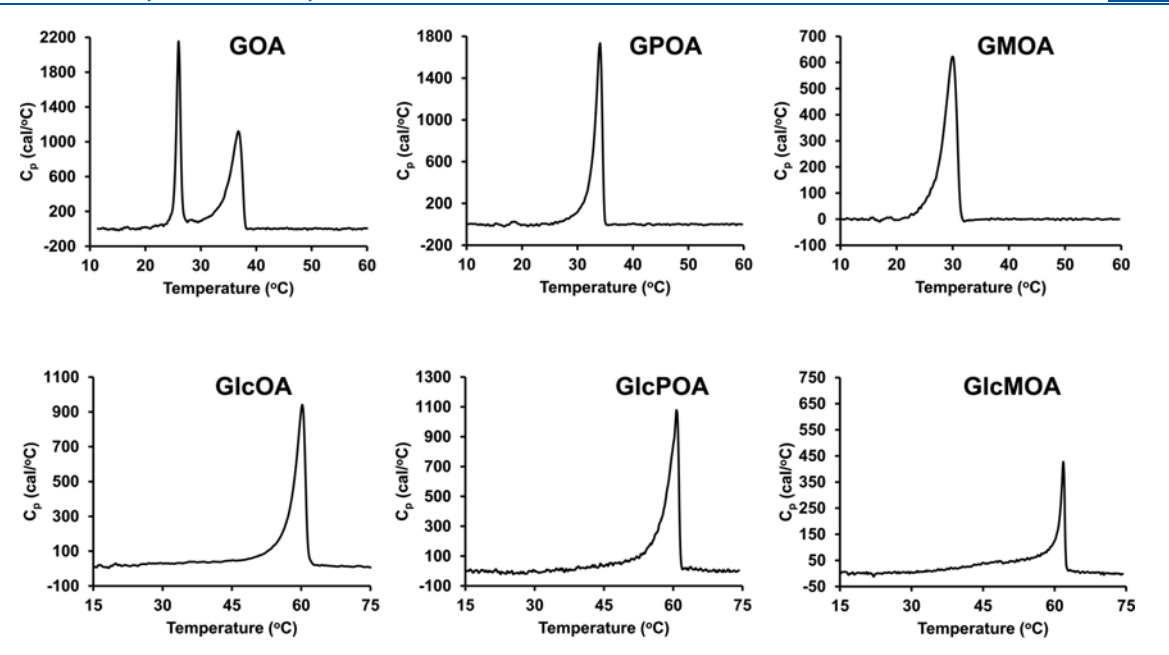


Figure 5. Characterization of the phase transition behavior by differential scanning calorimetry (DSC). DSC thermograms of aqueous dispersions of GOA (0.5 mM), GPOA (1 mM), GMOA (2 mM), GlcOA (0.5 mM), GPOA (0.5 mM), and GMOA (1.5 mM) at scan rate 30 °C/h.

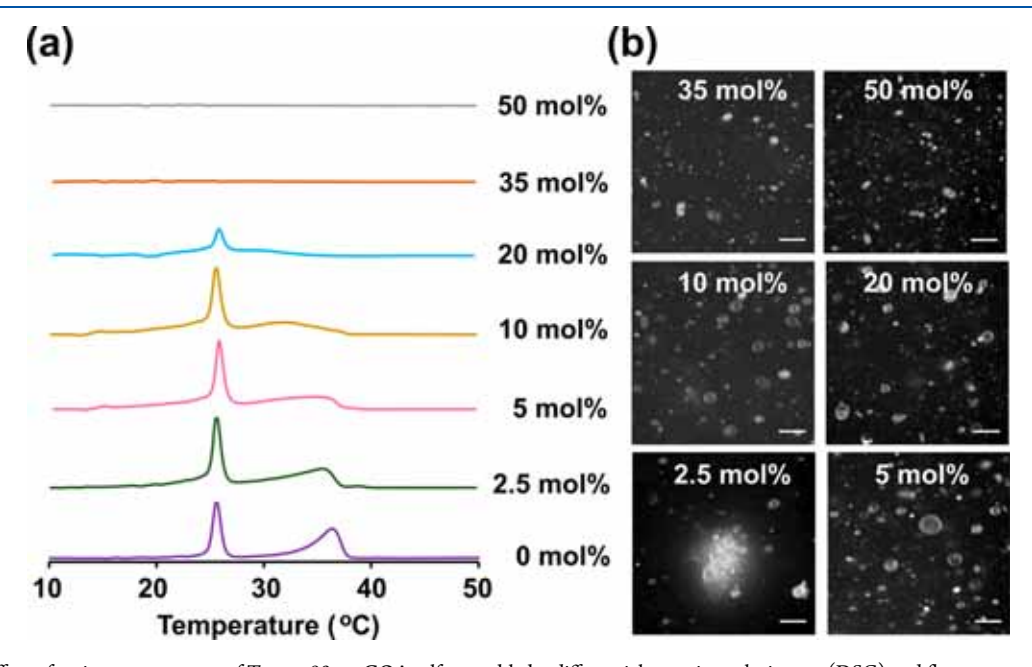


Figure 6. Effect of various percentages of Tween 80 on GOA self-assembly by differential scanning calorimetry (DSC) and fluorescence microscopy. (a) DSC thermograms of aqueous dispersions of a 0.5 mM GOA aqueous solution containing 0, 2.5, 5, 10, 20, 35, and 50 mol % of Tween 80 at scan rates of 30 °C/h. (b) Representative fluorescence microscopy images of GOA vesicles containing different percentages of Tween 80. Membranes were stained with Texas Red DHPE. All scale bars denote 10  $\mu$ m.

tations on the phase transition behavior in two kinds of selfassembled structures (vesicles and tubes), likely because of the chains are packed.

ween 80 on GOA Membranes. We next pdfelement line the effects of nonionic detergents on the and fluidity of GOA membranes. Various nts are used in liposomal preparations for drug

delivery to tune the fluidity and permeability properties of the

The Trial Version

membranes. 15 In particular, we studied the effects of the commercially available nonionic surfactant Tween 80 on GOA membranes using DSC (Figure 6a). Tween 80 is typically used in liposomal drug delivery systems as an "edge activator" or fluidity enhancer. 16-18 We obtained DSC thermograms of mixtures of GOA and Tween 80 at various molar ratios (0-50 mol % of Tween 80). The main transition peak broadened with increasing concentration of Tween 80, and at 35 mol % it

disappeared. Interestingly, the lower temperature peak decreased in intensity but retained its position and sharp features until it completely disappeared at 35 mol % Tween 80. We observed that Tween 80 significantly facilitated the hydration of GOA films into vesicles and improved its solubility in buffered solutions even when present at very low concentrations (2.5 mol %). This is likely because Tween 80 attenuates intermolecular hydrogen bonding between the galactose headgroups and alters the ordered water structure near the membrane surface. To support the data obtained from DSC, we observed the GOA vesicles formed with varying percentages of Tween 80 by microscopy (Figure 6b). As a general trend, we observed that with increasing percentage of Tween 80, the membranes were more fluid and dynamic (Figure S4) and the vesicles were smaller in size.

Encapsulation of Molecules of Various Sizes. For practical applications, it is highly important to know if the vesicles derived from  $\beta$ -D-galactopyranosylamide glycolipids can entrap molecules of biological relevance. Initially, we encountered some technical difficulties encapsulating molecules in GOA vesicles because of their relatively high main transition temperature (~37 °C). However, we observed that the inclusion of small quantities (6.25 mol %) of Tween 80 in the hydration buffer significantly improved the hydration and subsequent purification of the vesicles (Figure 7). This is likely due to the

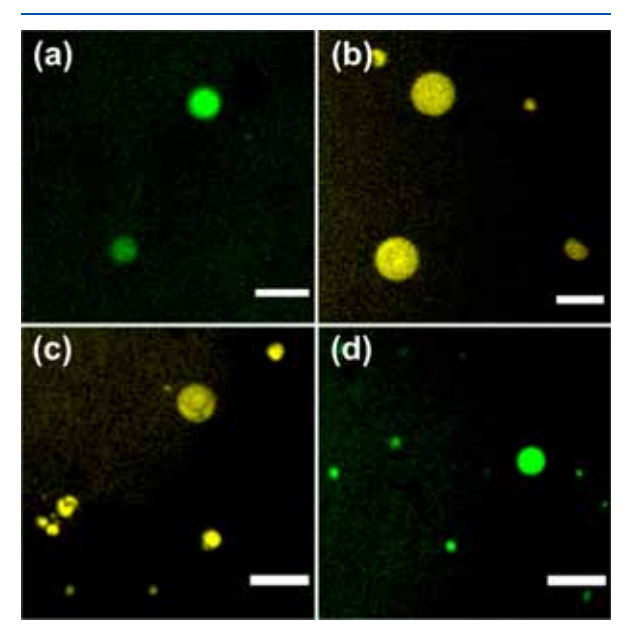


Figure 7. Encapsulation of various molecules in GOA vesicles. Spinning-disk confocal microscopy images of GOA vesicles encapsulating (a) HPTS (scale bar:  $10 \, \mu \text{m}$ ), (b) FITC-dextran (scale bar:  $5 \, \mu \text{m}$ ), (c) 5'-FAM dN<sub>20</sub> oligonucleotide (scale bar: 10  $\mu$ m), and (d) sfGFP (scale bar: 10  $\mu$ m). All vesicles were prepared with 3 mM GOA containing 6.25 mol % Tween 80.

combined effects of Tween 80 on the phase transition and or of **GOA**. At first, we encapsulated the polar nt dye 8-hydroxypyrene-1,3,6-trisulfonic acid **pdf**element ne) in GOA vesicles by the hydration method sicles with the encapsulated dye by spinning-The Trial Version roscopy (Figure 7a). This result suggested that ssible to encapsulate and retain biologically

relevant charged molecules such as nucleotide triphosphates in a

similar manner. Next, we attempted the encapsulation of FITClabeled dextran (3-5 kDa) and observed vesicles containing the same (Figure 7b). Subsequently, we could observe the encapsulation of a fluorescently labeled DNA oligonucleotide (Figure 7c) and the superfolder green fluorescent protein (sfGFP) (Figure 7d) in GOA vesicles. These results suggest that GOA vesicles can encapsulate and retain molecules relevant to biological systems. All of these properties could be extremely useful for several applications, such as the construction of cellmimetic vesicles.

Activity of  $\beta$ -Galactosidase Encapsulated in GOA Vesicles. Construction of cell-mimetics necessitates the encapsulation of proteins and other macromolecules in functional form. As a proof of concept demonstration, we chose the 540 kDa (tetramer) enzyme  $\beta$ -galactosidase as a model protein (Figure 8). At first, we hydrated a thin film of **GOA** with a buffer containing commercially available  $\beta$ galactosidase. Following this, we digested the unencapsulated  $\beta$ -galactosidase with proteinase K. Then, we added a fluorogenic substrate MUG and observed a continuous linear increase in the fluorescence from 4-methylumbelliferone ( $\lambda_{ex}$ : 375 nm,  $\lambda_{em}$ : 475 nm), the fluorescent product generated from MUG by  $\beta$ galactosidase. To verify that the observed activity is only from the encapsulated enzyme, we carried out a control experiment where proteinase K was added to the hydration buffer from the beginning. Upon the addition of MUG, we did not observe any increase in the fluorescence signal, suggesting that proteinase K digestion is effective and there is no residual activity from the cleaved fragments. These experiments suggest that the vesicles prepared with GOA can encapsulate biomacromolecules and allow the facile transport of small-molecule substrates across the membrane.

## CONCLUSIONS

We have explored in detail the self-assembly of single-chain  $\beta$ -Dglycopyranosylamide amphiphiles. We have shown that amphiphiles bearing a galactose headgroup are capable of selfassembly into vesicles, even when the identity of the unsaturated fatty acid chain is varied. Although lamellar phases have been observed in aqueous dispersions of various double-chain glycolipids, 1,3,19 reports of vesicle formation from single-chain glycolipids are rare. Moreover, it is likely that membranes derived from amphiphiles having various fatty acid chains will have different fluidity and permeability properties, and such properties may be exploited for applications in membrane mimetic chemistry. The observation that the identity of the monosaccharide group drastically influences the self-assembly properties opens avenues for the exploration of the properties of SCAs derived from other monosaccharides. It will also be interesting to study the consequences of other variations in the fatty acid chain, for instance, the introduction of branched chain fatty acids and hydroxylated fatty acids. Because the effect of stereochemical variations on structure and assembly is drastic in glycolipids compared with glycerophospholipids, it is highly likely that new properties could be discovered from various permutations of glycolipids.

The development of novel glycolipid amphiphiles may be beneficial for finding potential applications. We would like to point out that the syntheses of various  $\beta$ -D-glycopyranosylamides are straightforward and can be scaled up easily. This is largely because the  $\beta$ -D-glycopyranosylamine precursors are readily accessible from the corresponding sugars, 20,21 and various fatty acids are available from natural sources. Over the

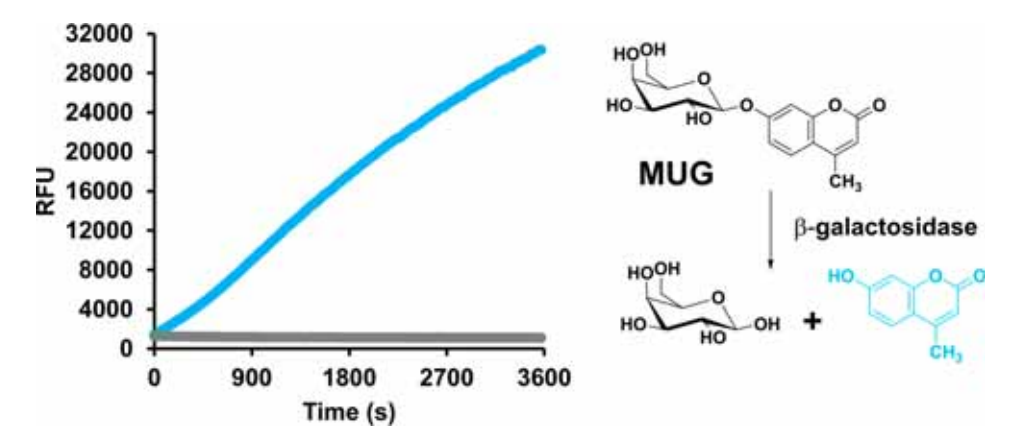


**Figure 8.** Activity of β-galactosidase encapsulated in **GOA** vesicles. Vesicles encapsulating β-galactosidase prepared by the hydration method were initially treated with proteinase K to digest unencapsulated proteins. Then, the substrate 4-methylumbelliferyl β-p-galactopyranoside (MUG) was supplied from the outside, and the enzymatic cleavage to the fluorescent product 4-methylumbelliferone was followed spectrofluorimetrically (blue trace). In a control experiment (gray trace), where proteinase K was added in the hydration buffer, no change in fluorescence was detected.

past few decades there has been increasing interest in using vesicles as a model system for artificial cells.<sup>22,23</sup> Single-chain glycolipid amphiphiles offer several advantages over more traditionally used SCAs such as fatty acids, especially in terms of a broader range of operating conditions (e.g., pH, presence of divalent cations, compatibility with biomolecules, etc.). In living organisms, glycolipids play an important role in macromolecular recognition, cell-cell adhesion, and immunogenicity. Such properties may be exploited to introduce novel functionalities into artificial cells. Single-chain glycolipids, being nonionic amphiphiles, are likely to be more benign to cells<sup>24</sup> than cationic lipids. Hence, they may be used in the development of vesicular drug delivery systems such as niosomes 15,25 and transferosomes.<sup>26</sup> Current efforts in our lab are focused on the development of more sophisticated applications of these glycolipid amphiphiles.

# ASSOCIATED CONTENT

# S Supporting Information

The Supporting Information is available free of charge on the ACS Publications website at DOI: 10.1021/acs.jpcb.9b01055.

NMR spectral images, Scheme S1, and Figures S1-S4 (PDF)

#### AUTHOR INFORMATION

#### **Corresponding Author**

\*E-mail: ndevaraj@ucsd.edu.

ORCID ®

The Trial Version

Roberto J. Brea: 0000-0002-0321-0156 Neal K. Devaraj: 0000-0002-8033-9973

utions

pdfelement was written through contributions of all ors have given approval to the final version of

The authors declare no competing financial interest.

### **Biography**



Photo courtesy: Erik Jepser

Neal K. Devaraj is a Professor of Chemistry and Biochemistry at the University of California, San Diego. He received a dual bachelor's degree in Chemistry and Biology from the Massachusetts Institute of Technology and a doctoral degree in Chemistry from Stanford University. His research group is interested in applying bioconjugation chemistry to problems in bottom-up synthetic biology, with a focus on developing synthetic cells. His research efforts have been recognized by the 2017 ACS Award in Pure Chemistry, the 2018 Blavatnik National Prize in Chemistry, and the 2019 Eli Lilly Award in Biological Chemistry.

## ACKNOWLEDGMENTS

This material is based on work supported by the National Science Foundation (CHE-1844346; Devaraj) and the U.S. Department of Energy (Biomolecular Materials Program, Division of Materials Sciences and Engineering) (DE-SC0018086; Sinha). We acknowledge Gabriel Ozorowski and Prof. Andrew Ward (The Scripps Research Institute) for their collaboration with the DSC measurements. We thank Henrike Niederholtmeyer for providing sfGFP. Roberto J. Brea thanks the Human Frontier Science Program (HFSP) for his Cross-Disciplinary Fellowship.

## REFERENCES

- (1) Hato, M.; Minamikawa, H.; Tamada, K.; Baba, T.; Tanabe, Y. Selfassembly of synthetic glycolipid/water systems. *Adv. Colloid Interface Sci.* **1999**, *80*, 233–270.
- (2) Schneider, M. F.; Zantl, R.; Gege, C.; Schmidt, R. R.; Rappolt, M.; Tanaka, M. Hydrophilic/hydrophobic balance determines morphology of glycolipids with oligolactose headgroups. *Biophys. J.* **2003**, *84*, 306–313.
- (3) Kitamoto, D.; Morita, T.; Fukuoka, T.; Konishi, M.; Imura, T. Self-assembling properties of glycolipid biosurfactants and their potential applications. *Curr. Opin. Colloid Interface Sci.* **2009**, *14*, 315–328.
- (4) Kitamoto, D. A.; Isoda, H.; Nakahara, T. Functions and potential applications of glycolipid biosurfactants from energy-saving materials to gene delivery carriers. *J. Biosci. Bioeng.* **2002**, *94*, 187–201.
- (5) Shimizu, T.; Minamikawa, H.; Kogiso, M.; Aoyagi, M.; Kameta, N.; Ding, W.; Masuda, M. Self-organized nanotube materials and their application in bioengineering. *Polym. J.* **2014**, *46*, 831–858.
- (6) Jung, J. H.; Rim, J. A.; Cho, E. J.; Lee, S. J.; Jeong, I. Y.; Kameda, N.; Masudae, M.; Shimizu, T. Stabilization of an asymmetric bolaamphiphilic sugar-based crown ether hydrogel by hydrogen bonding interaction and its sol-gel transcription. *Tetrahedron* **2007**, *63*, 7449–7456.
- (7) Brea, R. J.; Bhattacharya, A.; Bhattacharya, R.; Song, J.; Sinha, S. K.; Devaraj, N. K. Highly stable artificial cells from galactopyranose-derived single-chain amphiphiles. *J. Am. Chem. Soc.* **2018**, *140*, 17356–17360.
- (8) Kamiya, S.; Minamikawa, H.; Jung, J. H.; Yang, B.; Masuda, M.; Shimizu, T. Molecular structure of glucopyranosylamide lipid and nanotube morphology. *Langmuir* **2005**, *21*, 743–750.
- (9) Yen, T. F.; Gilbert, R. D.; Fendler, J. H. Advances in the Applications of Membrane-Mimetic Chemistry; Springer: New York, 1994.
- (10) Ma, Y.; Ghosh, S. K.; DiLena, D. A.; Bera, S.; Lurio, L.; Parikh, A. N.; Sinha, S. K. Cholesterol partition and condensing effect in phase-separated ternary mixture lipid multilayers. *Biophys. J.* **2016**, *110*, 1355–1366.
- (11) Budin, I.; Prywes, N.; Zhang, N.; Szostak, J. W. Chain-length heterogeneity allows for the assembly of fatty acid vesicles in dilute solutions. *Biophys. J.* **2014**, *107*, 1582–1590.
- (12) Chen, S. C.; Sturtevant, J. M.; Gaffney, B. J. Scanning calorimetric evidence for a third phase transition in phosphatidylcholine bilayers. *Proc. Natl. Acad. Sci. U. S. A.* **1980**, 77, 5060–5063.
- (13) Ruocco, M. J.; Shipley, G. G. Characterization of the subtransition of hydrated dipalmitoylphosphatidylcholine bilayers. *Biochim. Biophys. Acta, Biomembr.* **1982**, *691*, 309–320.
- (14) Saveyn, P.; Van der Meeren, P.; Zackrisson, M.; Narayanan, T.; Olsson, U. Subgel transition in diluted vesicular DODAB dispersions. *Soft Matter* **2009**, *5*, 1735–1742.
- (15) Kumar, G. P.; Rajeshwarrao, P. Nonionic surfactant vesicular systems for effective drug delivery an overview. *Acta Pharm. Sin. B* **2011**, *1*, 208–219.
- (16) El Zaafarany, G. M.; Awad, G. A. S.; Holayel, S. M.; Mortada, N. D. Role of edge activators and surface charge in developing ultradeformable vesicles with enhanced skin delivery. *Int. J. Pharm.* **2010**, 397, 164–172.
- (17) Khan, M. A.; Pandit, J.; Sultana, Y.; Sultana, S.; Ali, A.; Aqil, M.; Chauhan, M. Novel Carbopol-based transfersomal gel of 5-fluorouracil for skin cancer treatment: *In vitro* characterization and *in vivo* study. *Drug Delivery* **2015**, 22, 795–802.
- (18) Ahad, A.; Al-Saleh, A. A.; Al-Mohizea, A. M.; Al-Jenoobi, F. I.; Raish, M.; Yassin, A. E. B.; Alam, M. A. Formulation and
  - otion of Phospholipon 90 G and Tween 80 based ransdermal delivery of eprosartan mesylate. *Pharm.* 
    - Gama, Y.; Nagahora, H.; Yamaguchi, M.; Nakahara, The pH-sensitive conversion of rhamnolipid n. Lett. **1987**, 16, 763–766.

A.; Augé, J.; Drouillat, B. Improved synthesis of glycosylamines and a straightforward preparation of N-acylglycosyl-

- amines as carbohydrate-based detergents. Carbohydr. Res. 1995, 266, 211-219.
- (21) Sagar Reddy, G. V.; Rao, G. V.; Subramanyam, R. V. K.; Iyengar, D. S. A new novel and practical one pot methodology for conversion of alcohols to amines. *Synth. Commun.* **2000**, *30*, 2233–2237.
- (22) Bhattacharya, A.; Brea, R. J.; Devaraj, N. K. De novo vesicle formation and growth: an integrative approach to artificial cells. *Chem. Sci.* **2017**, *8*, 7912–7922.
- (23) Buddingh', B. C.; van Hest, J. C. M. Artificial cells: synthetic compartments with life-like functionality and adaptivity. *Acc. Chem. Res.* **2017**, *50*, 769–777.
- (24) Ernst, R.; Arditti, J. Biological effects of surfactants, IV. Effects of non-ionics and amphoterics on HeLa cells. *Toxicology* **1980**, *15*, 233–242.
- (25) Bartelds, R.; Nematollahi, M. H.; Pols, T.; Stuart, M. C. A.; Pardakhty, A.; Asadikaram, G.; Poolman, B. Niosomes, an alternative for liposomal delivery. *PLoS One* **2018**, *13*, No. e0194179.
- (26) Rai, S.; Pandey, V.; Rai, G. Transfersomes as versatile and flexible nano-vesicular carriers in skin cancer therapy: the state of the art. *Nano Rev. Exp.* **2017**, *8*, 1325708.